# Stimulus-evoked high frequency oscillations are present in neuronal networks on microelectrode arrays

**Chadwick M. Hales[1,2], Riley Zeller-Townson[2], Jonathan P. Newman[2], James T. Shoemaker[2], Nathan J. Killian[2] and Steve M. Potter[2]\***

[1] Department of Neurology, Center for Neurodegenerative Diseases, Emory University, Atlanta, GA, USA
[2] Laboratory for NeuroEngineering, Coulter Department of Biomedical Engineering, Georgia Institute of Technology, Atlanta, GA, USA

Pathological high frequency oscillations (250–600 Hz) are present in the brains of epileptic animals and humans. The etiology of these oscillations and how they contribute to the diseased state remains unclear. This work identifies the presence of microstimulation-evoked high frequency oscillations (250–400 Hz) in dissociated neuronal networks cultured on microelectrode arrays (MEAs). Oscillations are more apparent with higher stimulus voltages. As with *in vivo* studies, activity is isolated to a single electrode, however, the MEA provides improved spatial resolution with no spread of the oscillation to adjacent electrodes 200 μm away. Oscillations develop across four weeks *in vitro*. Oscillations still occur in the presence of tetrodotoxin and synaptic blockers, and they cause no apparent disruption in the ability of oscillation-presenting electrodes to elicit directly evoked action potentials (dAPs) or promote the spread of synaptic activity throughout the culture. Chelating calcium with ethylene glycol tetraacetic acid (EGTA) causes a temporal prolongation of the oscillation. Finally, carbenoxolone significantly reduces or eliminates the high frequency oscillations. Gap junctions may play a significant role in maintaining the oscillation given the inhibitory effect of carbenoxolone, the propagating effect of reduced calcium conditions and the isolated nature of the activity as demonstrated in previous studies. This is the first demonstration of stimulus-evoked high frequency oscillations in dissociated cultures. Unlike current models that rely on complex *in vivo* recording conditions, this work presents a simple controllable model in neuronal cultures on MEAs to further investigate how the oscillations occur at the molecular level and how they may contribute to the pathophysiology of disease.

**Keywords: multielectrode array, microelectrode, MEA, oscillation, gap junction, NeuroRighter, carbenoxolone, microstimulation**

## INTRODUCTION

The complex process of cognition at a very elementary level is subserved by the transmission of signals across synapses between neurons. These signals often accumulate and produce rhythms or oscillations. For over half a century, lower frequency oscillations (δ:1–3 Hz, θ:4–7 Hz, α:8–12 Hz, β:13–20 Hz) have been routinely analyzed as part of an electroencephalogram (EEG) and utilized to evaluate superficial cortical dysfunction. Oscillations in the γ range (20–80 Hz) have been implicated in memory storage as well as more general brain synchronization in response to stimuli (Engel and Singer, 2001; Fell et al., 2001, 2003; Sederberg et al., 2003; Gruber et al., 2004; Herrmann et al., 2004; Axmacher et al., 2008). The relationship of frequencies above 80 Hz to brain function and pathology is currently the topic of much study.

High frequency oscillations above 80 Hz have been described in animal models as well as humans and are commonly divided into two categories: ripples (80–250 Hz) and fast ripples (250–600 Hz) (Buzsaki et al., 1992; Chrobak and Buzsaki,

1996; Bragin et al., 1999a, 2010; Staba et al., 2004; Ulanovsky and Moss, 2007). Other subdivisions within frequency ranges are also utilized when describing oscillations. For example, sharp-wave ripple complex is a term used to delineate oscillations 140–200 Hz (Behrens et al., 2005). Most studies with recordings from behaving animals show that ripple frequency oscillations are involved in memory formation and consolidation with a few studies suggesting that these oscillations may function as a seizure nidus (Siapas and Wilson, 1998; Sirota et al., 2003; Axmacher et al., 2008; Engel et al., 2009; Bragin et al., 2010). Fast ripples, however, are almost uniformly associated with epileptogenesis.

These fast ripples have been observed in rats that have spontaneous seizures and are thought to be pathological given their association with brain regions displaying seizure onset (Bragin et al., 1999b,c, 2000). This phenomenon has been observed with hippocampal seizure onset and there is data that correlates areas with greater numbers of fast ripples and increased seizure rates (Bragin et al., 2003, 2005). Fast ripples may even be a predictive measure for seizures (Bragin et al., 2004). Finally, many

studies have demonstrated the presence of fast ripples in epileptic patients (Bragin et al., 1999b, 2002b; Staba et al., 2002, 2004; Jirsch et al., 2006; Urrestarazu et al., 2007; Jacobs et al., 2008; Khosravani et al., 2009).

The underlying cause of these fast ripples or pathological high frequency oscillations is not entirely clear. Whereas ripple oscillations may represent the accumulation of inhibitory post-synaptic potentials, the pathological high frequency oscillations or fast ripples may represent a small population of bursting cells (Bragin et al., 2002a, 2007; Engel et al., 2009). However, there is also data suggesting that electrical coupling through gap junctions may be partially responsible for the ripple oscillations (Draguhn et al., 1998; Traub et al., 2002; Roopun et al., 2010).

Given the implication of high frequency oscillations in epileptogenesis and the prevalence of epilepsy, it is unfortunate that models for studying the phenomenon are limited. Recent work by Cardin and colleagues demonstrated the ability to generate gamma oscillations by activating fast spiking interneurons utilizing optogenetic techniques, however, this is limited to much lower frequencies (∼40 Hz) (Cardin et al., 2009). Another group was able to produce sharp-wave ripple complexes in hippocampal slice cultures through stimulation protocols that evoke long-term potentiation (Behrens et al., 2005). Although epileptic rats and humans have fast ripples, there are significant challenges in using these models that rely on implanted electrodes to study cellular and molecular changes.

Our laboratory utilizes dissociated neuronal networks on microelectrode arrays (MEAs) to study learning and network dynamics (Wagenaar et al., 2005, 2006a; Rolston et al., 2007; Bakkum et al., 2008; Chao et al., 2008; Hales et al., 2010). Neuronal networks on MEAs have several advantages over other electrophysiological techniques (Potter and DeMarse, 2001). Entire networks of neurons can be monitored instead of single neurons as with patch clamping. Unlike voltage clamping experiments, cultures can be studied for weeks to months since cells are not damaged during recording. Another advantage for cultures on MEAs is that there is notable ease in manipulating these networks from both pharmacological and genetic avenues and cultures of different sizes down to single cells can be followed in real time with imaging. Like slice cultures and *in vivo* preparations, neuronal networks on MEAs maintain a high level of complexity in the mature state and exhibit complex recurring activity patterns (Wagenaar et al., 2006a; Madhavan et al., 2007; Pimashkin et al., 2011). Glutamate and GABA are the main excitatory and inhibitory neurotransmitters in these neuronal networks (Dichter, 1978). However, unlike slice cultures and whole animals, neuronal networks on MEAs represent a far simpler and more reductionist model for experimentation.

In this work we were able to induce fast ripple oscillations (250–400 Hz) in neuronal networks on MEAs *in vitro* with extracellular stimulation. Supporting experiments in this work suggest that these fast ripples may be mediated by gap junctions. This work is the first to demonstrate high frequency oscillations in dissociated cells forming neuronal networks. The model could be developed to study epileptogenesis and perhaps even be used in a translational approach for evaluating efficacy of pharmacological therapies.

## MATERIALS AND METHODS
### CELL CULTURE TECHNIQUES
Cells were prepared and plated onto MEAs as described (Potter and DeMarse, 2001; Hales et al., 2010). Briefly, hippocampi and cortical hemispheres were obtained from E18 rat embryos and placed into medium following protocols in adherence to federal and institutional guidelines. In separate tubes, hippocampi and cortical hemispheres were digested with trypsin, triturated, and filtered (40 μm) (Hales et al., 2010). MEAs were sterilized with 70% ethanol soak followed by ultraviolet light exposure in a biological safety cabinet. The MEA culturing surface was prepared with polyethylenimine, followed by three water washes, drying, then laminin coating of the MEA center ensuring to cover all electrodes. 50,000 cells were used for each dish (5000–10,000 cells/mm$^2$). Culturing medium [90 ml Dulbecco's modified Eagle's medium (Irvine Scientific 9024), 10 ml horse serum (Gibco 16050), 1 ml sodium pyruvate (100 mM, Gibco 11360), 250 μl GlutaMAX (Gibco 35050), and insulin (final concentration 2.5 μg/ml, Sigma I-5500)] was changed in its entirety on day one *in vitro*. Subsequent culture feeding occurred every 3–4 days *in vitro* (DIV) and involved removing half the medium in the dish and replacing with fresh medium. Cultures were incubated at 35°C with 5% carbon dioxide, 9% oxygen, and 65% relative humidity (Potter and DeMarse, 2001).

### MEA RECORDING AND STIMULATION
MEAs (59 titanium nitride electrodes, 30 μm diameter, 200 μm interelectrode spacing, one ground electrode, with glass culturing well) were purchased from Multichannel Systems. The recording system, NeuroRighter, included custom software and hardware as described previously (http://code.google.com/p/neurorighter/) (Rolston et al., 2009, 2010). The recording apparatus utilized a MEA60 Multichannel Systems preamplifier for docking the MEA. All recordings took place in the culture incubator at 35°C with 5% carbon dioxide, 9% oxygen, and 65% relative humidity (Potter and DeMarse, 2001). Dishes were allowed to equilibrate for 5–10 min in incubator atmosphere prior to recording since previous observations suggest that culture movement causes a transient reduction in culture wide firing (Wagenaar et al., 2006b). Extracellular stimulation involved the sequential delivery of biphasic square wave voltage controlled pulses, positive phase first (400 μs/phase), randomly across all electrodes at 1 Hz. Stimulation voltages ranged from ±0.3 V to ±0.7 V. Raw electrode voltages were sampled at 25 kHz and band-pass filtered with a second order Butterworth with 3 dB roll-off frequencies of 200 and 5000 Hz. Amplifier gain was set at 1200. Extracellular action potentials were detected as voltage transients exceeding six times the estimated root-mean-square (RMS) noise levels for each electrode. The SALPA algorithm, a fast, local polynomial curve fitter, was used for rapid recovery from stimulation artifacts (Wagenaar and Potter, 2002). Data presented are representative SALPA traces, raster plots, and power spectra from a total of 173 electrodes exhibiting a stimulus-induced oscillation, across nine cultures (six hippocampal, three cortical) from three different plating sessions. Recordings were obtained from cultures 3–8 weeks *in vitro* unless otherwise indicated in the figure legends. Cultures utilized for the experiments

were assessed for spontaneous and stimulus-evoked activity twice weekly.

### PHARMACOLOGICAL ADMINISTRATION

Drugs were added to the MEA via medium exchange, utilizing the medium conditioned by the culture. The exchange was conducted in the biological safety cabinet and medium was filtered (0.2 μm) to maintain sterility in the culture. Mock exchanges were also conducted as a control to ensure the pharmacological effect was not due to movement-induced changes in firing properties from the exchange or transporting the dish about the room. Final concentrations of pharmacological agents (all from Sigma): carbenoxolone (CBX, 150 μM), EGTA (10 μM), tetrodotoxin (TTX, 1 μM), 6-cyano-7-nitroquinoxaline-2,3-dione (CNQX, 20 μM), amino-5-phosphonovaleric acid (APV, 10 μM), bicuculline (20 μM).
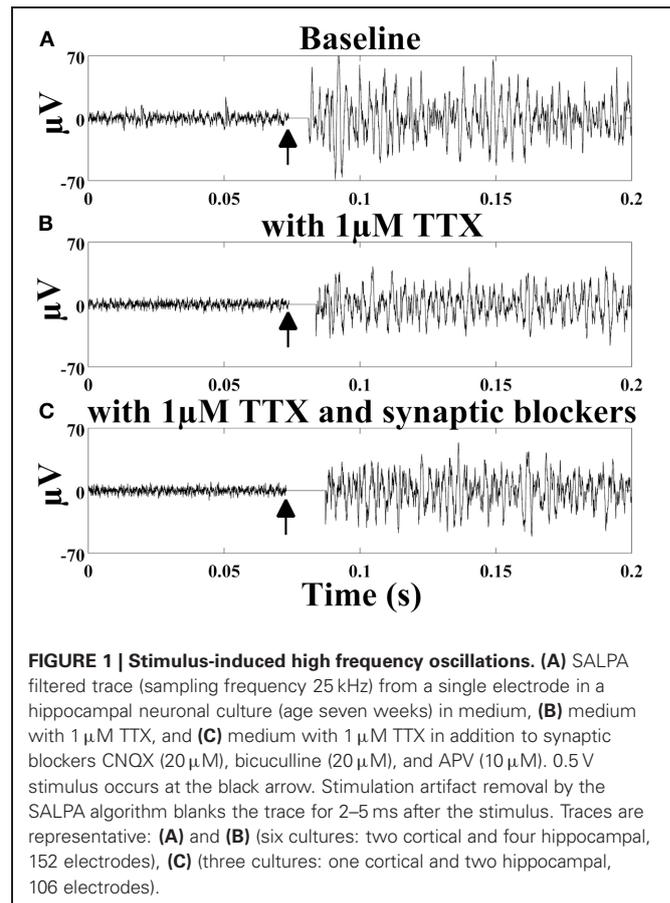
### DATA ANALYSIS

All data analysis was conducted using MATLAB. NeuroRighter output files were imported into MATLAB using conversion tools freely available on the NeuroRighter code site. Student's $t$-test was utilized to determine statistical significance with standard deviation represented with all statistical analysis as indicated. Power spectrum plots were created using the Field-Trip toolbox in MATLAB (Oostenveld et al., 2011) and calculated by averaging the average power of two stimulus trials for each electrode across multiple cultures for the given conditions as described in the results.

## RESULTS

### EXTRACELLULAR STIMULATION INDUCES HIGH FREQUENCY OSCILLATIONS ON SINGLE MEA ELECTRODES

Previous studies in hippocampal slice cultures demonstrated the ability to elicit high frequency oscillations with electrical stimulation (Draguhn et al., 1998; Behrens et al., 2005). The NeuroRighter recording system is ideal for analyzing post stimulus spike data and activity traces to search for these oscillations because it employs the SALPA algorithm which allows for rapid recovery from stimulus-induced artifacts (Wagenaar and Potter, 2002; Rolston et al., 2009). This provides voltage traces within 2–5 ms post stimulus.

Sequential random stimulation at 1 Hz across electrodes of MEAs supporting hippocampal neuronal networks allowed us to identify electrodes that display a stimulus-evoked high frequency oscillation (**Figure 1A**). This oscillation was still present even when cell medium contained 1 μM TTX (**Figure 1B**), blocks voltage-dependent sodium channels and eliminates spiking. AMPA, NMDA, and GABA receptor antagonists CNQX, APV, and bicuculline, respectively, did not disrupt the oscillation (**Figure 1C**). Oscillations were also present in cortical neuronal cultures (**Figure 3A**) and similarly affected by pharmacological manipulation. The spectral content of the oscillations was calculated over sliding time windows after the stimulus. Average power spectra are presented in **Figure 2**. The robust oscillation was not present under baseline conditions as represented by the average power spectrum of the oscillation-containing electrode when stimulation occurs on other electrodes (**Figure 2A**; from $n = 152$



**FIGURE 1 | Stimulus-induced high frequency oscillations. (A)** SALPA filtered trace (sampling frequency 25 kHz) from a single electrode in a hippocampal neuronal culture (age seven weeks) in medium, **(B)** medium with 1 μM TTX, and **(C)** medium with 1 μM TTX in addition to synaptic blockers CNQX (20 μM), bicuculline (20 μM), and APV (10 μM). 0.5 V stimulus occurs at the black arrow. Stimulation artifact removal by the SALPA algorithm blanks the trace for 2–5 ms after the stimulus. Traces are representative: **(A)** and **(B)** (six cultures: two cortical and four hippocampal, 152 electrodes), **(C)** (three cultures: one cortical and two hippocampal, 106 electrodes).

electrodes). There was a band of increased power between 250 Hz and 400 Hz (**Figure 2B**; $n = 152$ electrodes) that persisted in the presence of 1 μM TTX (**Figure 2C**; 106 electrodes). There was no statistical difference in the oscillation duration ($2.40 \pm 2.22$ s vs. $2.89 \pm 2.50$ s; $p$-value $= 0.09$) between untreated cultures and cultures with TTX (**Table 1**). The oscillation amplitude was $25.63 \pm 7.97$ μV in TTX treated cultures while accurate amplitudes could not be determined for oscillations in untreated cultures because of superimposed action potentials. A less intense band of increased power was noted just above 600 Hz.

The oscillation was voltage-dependent since it was absent with stimulation at 0.3 V but present at higher voltages (**Figure 3A**). The duration of the oscillation increased from no oscillation at 0.3 V $-3.53 \pm 2.86$ s with 0.5 V stimulus and $7.38 \pm 3.61$ s with 0.7 V stimulus (**Figure 3B**). The increase in duration from 0.5 V to 0.7 V was statistically significant ($p < 0.001$). To ensure that the oscillation was not caused by a stimulation artifact or issue with hardware, stimulation on a commercially available test MEA (with resistors and capacitors to represent electrode impedance) in addition to a MEA without cells did not reproduce the oscillation (data not shown). Also, it could not be observed on every electrode of an MEA. MEAs were cultured to uniform density so as to control for variability that could be introduced by differences in cellular contacts with electrodes. MEAs were visually inspected to ensure a uniform distribution with each recording session.
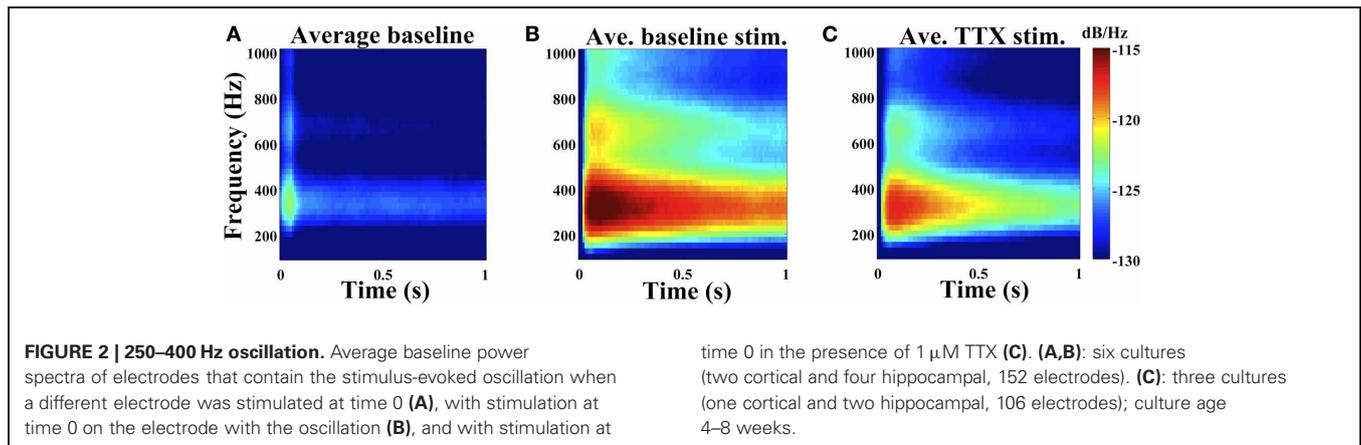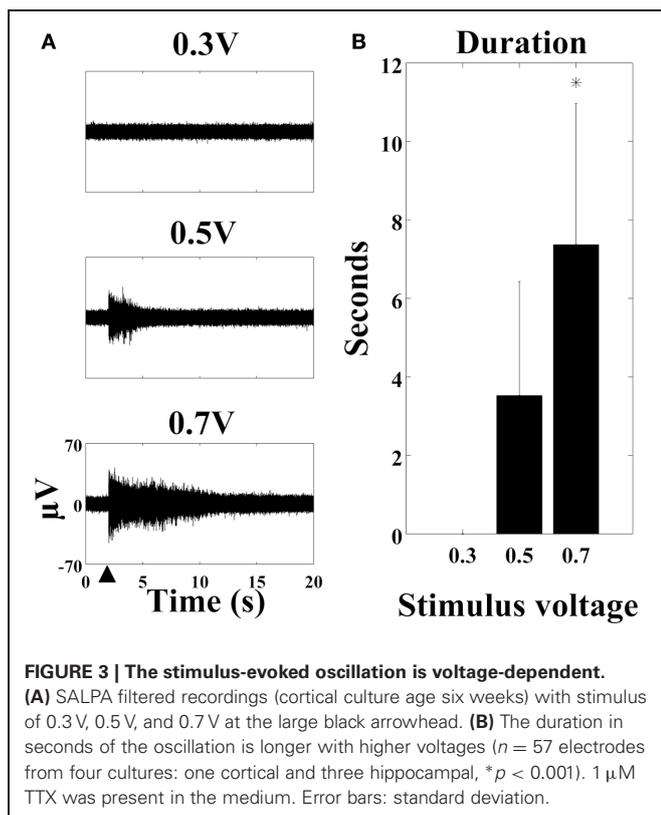
**FIGURE 2 | 250–400 Hz oscillation.** Average baseline power spectra of electrodes that contain the stimulus-evoked oscillation when a different electrode was stimulated at time 0 **(A)**, with stimulation at time 0 on the electrode with the oscillation **(B)**, and with stimulation at time 0 in the presence of 1 µM TTX **(C)**. **(A,B)**: six cultures (two cortical and four hippocampal, 152 electrodes). **(C)**: three cultures (one cortical and two hippocampal, 106 electrodes); culture age 4–8 weeks.

**Table 1 | Mean amplitude and duration of stimulus-evoked oscillation.**

| Culture condition | Mean max amplitude (µV) ± SD | Mean oscillation duration (sec) ± SD | Condition comparison | Mean max amplitude (p-value)*** | Oscillation duration (p-value)*** |
|---|---|---|---|---|---|
| Untreated | N/A[a] | 2.40 ± 2.22 | Untreat./TTX | N/A[a] | 0.09 |
| TTX | 25.63 ± 7.97 | 2.89 ± 2.50 | TTX/CBX | $2.26 \times 10^{-23}$ | $1.97 \times 10^{-16}$ |
| CBX | 16.05 ± 4.87 | 0.73 ± 0.87 | TTX/EGTA | 0.23 | $1.13 \times 10^{-136}$ [b] |
| EGTA | 23.38 ± 9.98 | >60[b] | | | |

[a] Unable to accurately determine amplitude with superimposed action potentials.

[b] Duration of oscillation was longer than stimulus interval (60 s) between stimulation trials on a given channel. Sixty seconds duration for the oscillation was utilized for calculating the p-value.

*** p-value < 0.05 designates statistical significance.



**FIGURE 3 | The stimulus-evoked oscillation is voltage-dependent.** **(A)** SALPA filtered recordings (cortical culture age six weeks) with stimulus of 0.3 V, 0.5 V, and 0.7 V at the large black arrowhead. **(B)** The duration in seconds of the oscillation is longer with higher voltages ($n = 57$ electrodes from four cultures: one cortical and three hippocampal, *$p < 0.001$). 1 µM TTX was present in the medium. Error bars: standard deviation.

Previous microwire studies in rodents and epileptic humans showed that similar high frequency oscillations are isolated to single microwires with around 1 mm spacing (Bragin et al., 2003; Schevon et al., 2009). The work here suggested a very localized population of cells is responsible for the activity. The stimulus-evoked oscillations in cultured networks were present only on the single stimulation electrode with no spread to adjacent electrodes (**Figure 4**), even with higher voltages (data not shown). These results provide improved spatial resolution of the activity compared to *in vivo* microwire studies since the oscillation was further localized to a population of cells within a 200 µm radius.

**STIMULUS-EVOKED OSCILLATIONS DEVELOP OVER TIME**

Cultures on MEAs mature as neurons progress from a dissociated state to highly connected neuronal networks with millions of synapses (Wagenaar et al., 2006b). If the stimulus-evoked high frequency oscillations were caused by single cells, then the activity may be more readily apparent very early in development. However, if the oscillations developed and strengthened over time, then this could suggest dependency on network connections. The power spectrum at 11 DIV showed limited development of the 250–400 Hz oscillations, however, high frequency oscillations are present by 18 DIV and persist through 27 DIV (**Figure 5A**, average power spectra from 26 electrodes, four cultures). The number of electrodes with this stimulus-evoked oscillation varied between cultures ($n = 7$) and increased from no clear oscillations at 1.5 weeks, to $8.71 \pm 7.59\%$ of electrodes with
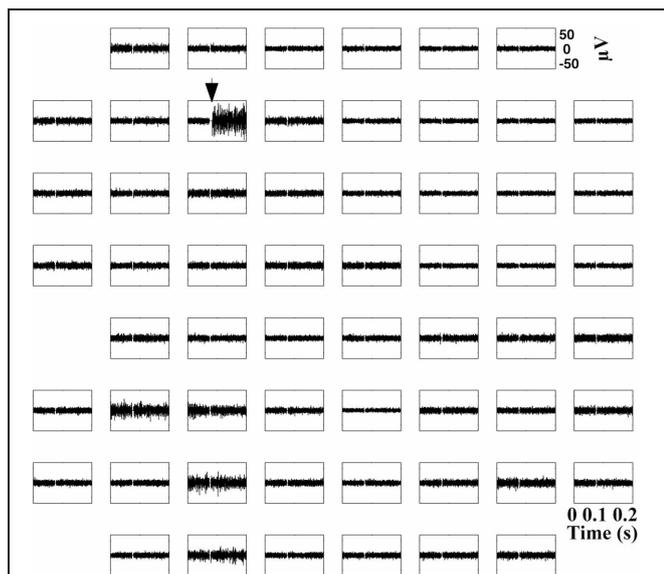
**FIGURE 4 | Oscillations are isolated to a single electrode.** 200 ms of SALPA filtered traces appropriately oriented to each of 59 electrodes (200 μm spacing) from a single microelectrode array. 0.5 V stimulus occurs only on the electrode with the black arrow. Representative example (hippocampal culture age six weeks) from n = 152 electrodes in six cultures (two cortical and four hippocampal). TTX was not present in the medium.
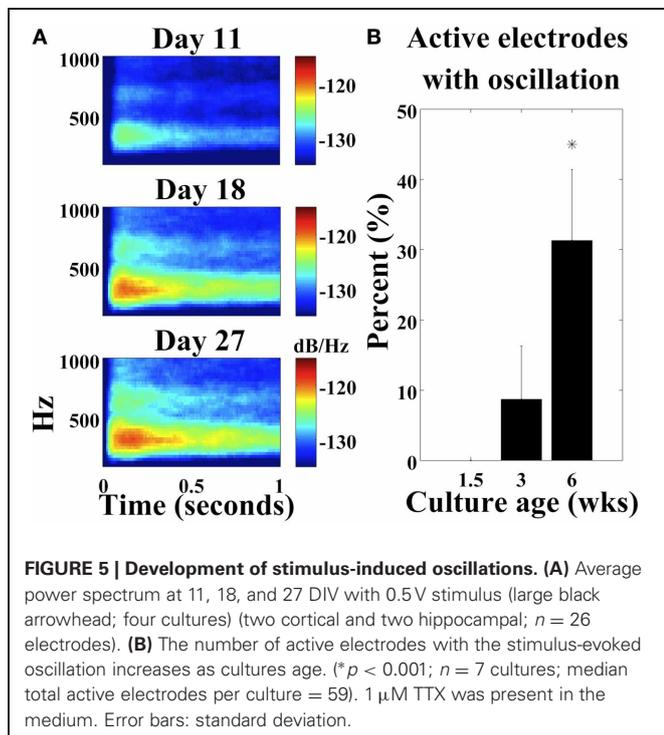


**FIGURE 5 | Development of stimulus-induced oscillations. (A)** Average power spectrum at 11, 18, and 27 DIV with 0.5 V stimulus (large black arrowhead; four cultures) (two cortical and two hippocampal; n = 26 electrodes). **(B)** The number of active electrodes with the stimulus-evoked oscillation increases as cultures age. (*p < 0.001; n = 7 cultures; median total active electrodes per culture = 59). 1 μM TTX was present in the medium. Error bars: standard deviation.

the oscillation at three weeks, and $31.25 \pm 10.13\%$ of electrodes with the oscillation at six weeks (**Figure 5B**). Results in **Figure 5B** were calculated based on increasing amplitudes, however, the power spectrum in **Figure 5A** suggests that subtle findings of the oscillation are even becoming apparent at Day 11.
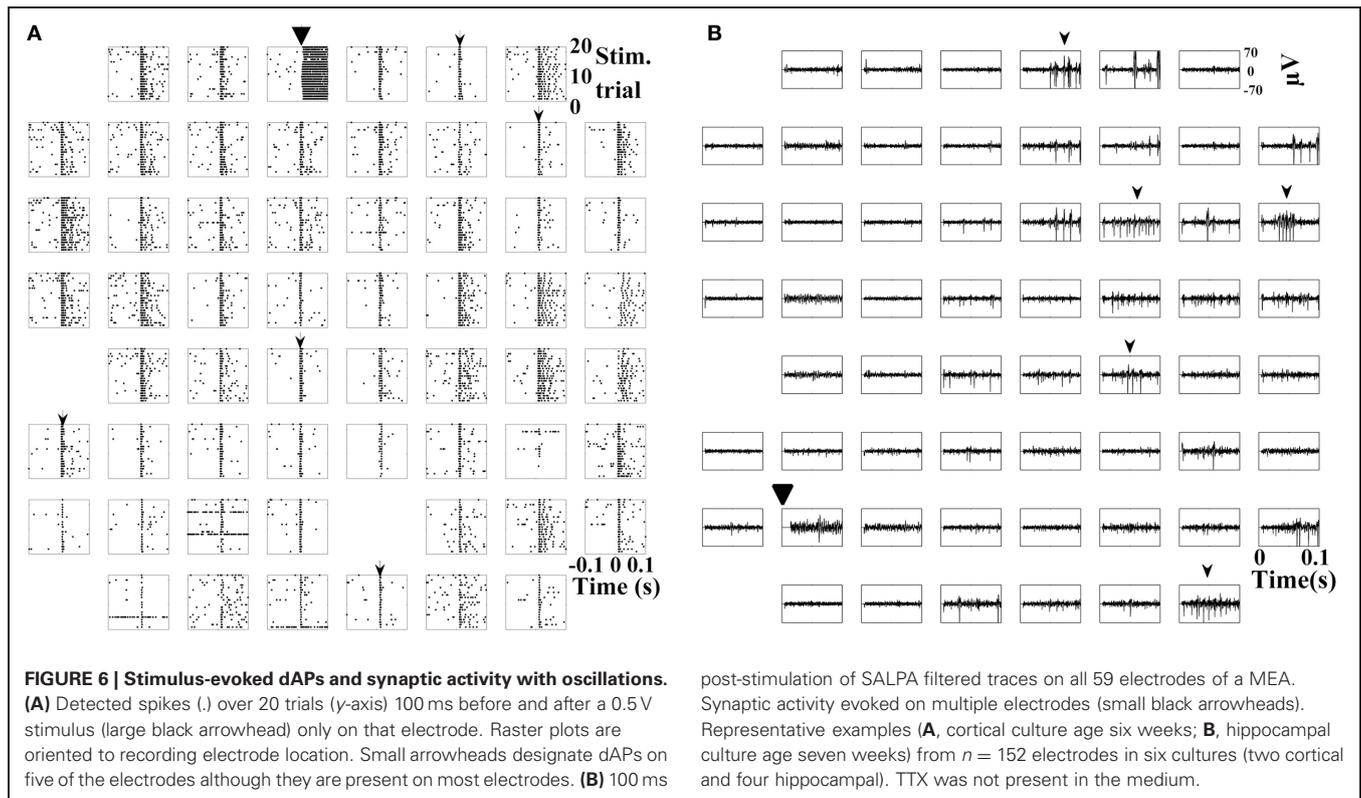
## dAPs AND SYNAPTIC ACTIVITY PERSIST DESPITE THE OSCILLATION

In addition to oscillations, typical stimulus-evoked activity on MEAs includes evoked spiking activity. Directly evoked action potentials (dAPs), which are detected even in the presence of synaptic blockers, occur first followed by a synaptic wave spreading across the dish (Wagenaar et al., 2006b; Bakkum et al., 2008). dAPs are spikes that occur in the first 0–20 ms after a stimulus and represent a direct depolarization of a cell process or soma by the stimulating electrode. dAPs are best demonstrated on spike raster plots containing multiple stimulus trials because their latency has little variation making them more visible as aligned spikes when plotted on the same graph (**Figure 6A**). **Figure 6A** shows that despite evoking a robust oscillation on one electrode, dAPs continued to occur throughout the culture, and this is similar to dAPs produced by electrodes that do not display the evoked oscillation (data not shown). Similarly, there was also no clear disruption of stimulus-evoked synaptic activity (**Figure 6B**). There were action potentials present on most electrodes within 100 ms of the stimulus.

## THE EFFECT OF PHARMACOLOGICAL BLOCKADE AND REDUCED CALCIUM CONDITIONS ON STIMULUS-EVOKED OSCILLATIONS IN MEAs

Previous work has suggested that ripples around 200 Hz may be due to direct electrical coupling (Draguhn et al., 1998; Traub et al., 2002; Roopun et al., 2010). Modeling data by the same group suggested that these types of junctions are theoretically capable of producing 200 Hz oscillations in local neuron populations (Draguhn et al., 1998). The frequency of fast ripples is likely greater than what is physiologically possible for an action potential train from a single neuron. Multi-unit action potentials are possible, however, one would expect spread of the oscillation to other electrodes in the MEA when there is no pharmacological blockade. This spread does was not observed (**Figures 4** and **6**). Pharmacological blockade of voltage-dependent sodium channels with tetrodotoxin failed to quell the stimulus-evoked high frequency oscillation (**Figure 1B**). Direct synaptic blockade also had no effect on the stimulus-evoked oscillation (**Figure 1C**). The addition of carbenoxolone (CBX, 150 μM), a putative gap junction blocker, either reduced the amplitude and duration of the stimulus-evoked oscillation or completely abolished the oscillation (**Figure 7A**). Average power spectra demonstrated a near complete loss of the oscillation when comparing cultures containing 1 μM TTX (**Figure 7B**) to cultures containing 1 μM TTX plus 150 μM CBX (**Figure 7C**). CBX reduced the oscillation amplitude from an average $25.63 \pm 7.97$ μV to $16.05 \pm 4.87$ μV with a $p$-value of $2.26 \times 10^{-23}$ while the oscillation duration was reduced from $2.89 \pm 2.50$ s to $0.73 \pm 0.87$ s with a $p$-value of $1.97 \times 10^{-16}$ (**Table 1**). The oscillation returned to baseline with CBX washout.

Previous studies showed that gap junction activity is potentiated in low calcium conditions (Jiruska et al., 2010), and there is a model of epilepsy based on this premise (Perez-Velazquez et al., 1994). In this work, low extracellular calcium conditions induced by chelating the calcium in the medium with EGTA, enhanced the stimulus-evoked oscillation with significantly prolonged oscillation durations (**Figure 8A** and **Table 1**). The oscillation persisted

FIGURE 6 | Stimulus-evoked dAPs and synaptic activity with oscillations.
(A) Detected spikes (.) over 20 trials (y-axis) 100 ms before and after a 0.5 V stimulus (large black arrowhead) only on that electrode. Raster plots are oriented to recording electrode location. Small arrowheads designate dAPs on five of the electrodes although they are present on most electrodes. (B) 100 ms post-stimulation of SALPA filtered traces on all 59 electrodes of a MEA. Synaptic activity evoked on multiple electrodes (small black arrowheads). Representative examples (A, cortical culture age six weeks; B, hippocampal culture age seven weeks) from n = 152 electrodes in six cultures (two cortical and four hippocampal). TTX was not present in the medium.

into the next stimulus trial on electrodes tested, so by using an average time of sixty seconds between trials as a conservative estimate, the calculated p-value was highly significant at $1.13 \times 10^{-113}$. The amplitude of the oscillation was unchanged ($p = 0.23$). The stimulus-evoked oscillation returned to a baseline duration following washout (**Figure 8A**). The average power spectrum showed a slight narrowing of the 250–400 Hz power band (**Figures 8B and 8C**). Therefore, this oscillation-potentiating effect induced by EGTA provided further support that gap junctions may be responsible for the stimulus-evoked oscillation.
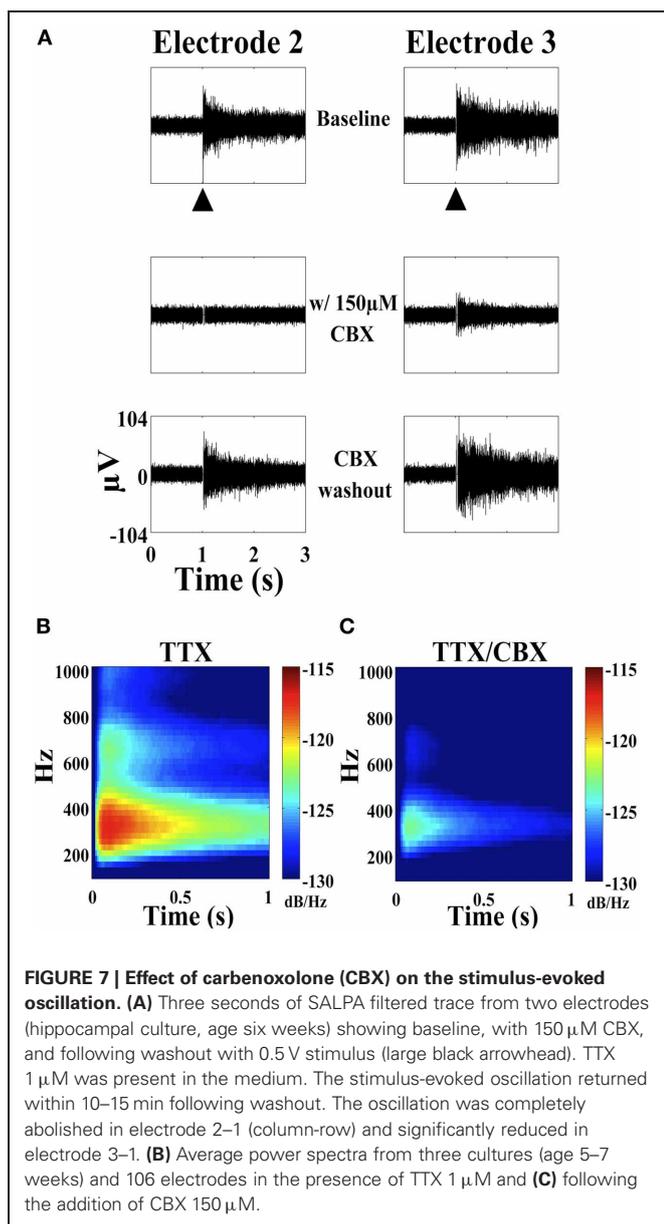
## DISCUSSION

High frequency oscillations likely have various functional capacities in the human brain. Although gamma and ripple (sharp-wave ripple) frequencies may represent normal oscillatory behavior that subserves regional synchronization and memory consolidation, the fast ripple frequencies seem to be connected with a pathological state (Buzsaki et al., 1992; Chrobak and Buzsaki, 1996; Siapas and Wilson, 1998; Bragin et al., 1999a,b, 2010; Engel and Singer, 2001; Sirota et al., 2003; Staba et al., 2004; Ulanovsky and Moss, 2007; Engel et al., 2009). Establishing a model to more closely assess the underlying etiology of such fast ripples could provide valuable information about the genesis of diseases like epilepsy as well as establish more foundational knowledge that could apply to other types of network oscillations. We present data on such an ideal model showing stimulus-evoked high frequency oscillations in neuronal networks on MEAs.

The accessibility of cultures on MEAs for manipulation is a key benefit of this model. Once an electrode with the oscillation is identified, the oscillation can be followed for weeks. This would allow for pharmacological manipulation in addition to more complex genetic studies such as transfecting with a desired gene or knocking down an RNA message. More detailed imaging work is also feasible and would be needed to further characterize molecular underpinnings of the oscillation. Finally, the ability to monitor the entire network with other electrodes allows for a more global picture than could be seen with single-cell electrophysiology. Although no clear immediate difference in network response was detected when looking at direct evoked action potentials and the effect on synaptic activity, future studies could assess longer lasting changes in network activity and dynamics. As with any model, there are also disadvantages and in particular here, networks likely do not completely reconnect and fully recapitulate *in vivo* neuronal organization. However, since networks must mature and presumably form various connections for the stimulus-evoked oscillation to be present, this work suggests that some degree of architectural preservation must occur in dissociated neuronal networks on MEAs.

The frequency of 250–400 Hz suggests that the oscillations are likely pathological and although this could be a function of how neuronal networks form *in vitro*, many of the characteristics of the oscillations are similar to those observed from macro- and microwire studies *in vivo* (Bragin et al., 1999b,c, 2002b, 2010; Staba et al., 2002; Jirsch et al., 2006; Urrestarazu et al., 2007; Jacobs et al., 2008; Worrell et al., 2008; Khosravani et al., 2009). Most notable is the fact that the stimulus-evoked oscillations are isolated to single electrodes suggesting that a highly localized population of cells is likely responsible as mentioned

FIGURE 7 | Effect of carbenoxolone (CBX) on the stimulus-evoked oscillation. (A) Three seconds of SALPA filtered trace from two electrodes (hippocampal culture, age six weeks) showing baseline, with 150 μM CBX, and following washout with 0.5 V stimulus (large black arrowhead). TTX 1 μM was present in the medium. The stimulus-evoked oscillation returned within 10–15 min following washout. The oscillation was completely abolished in electrode 2–1 (column-row) and significantly reduced in electrode 3–1. (B) Average power spectra from three cultures (age 5–7 weeks) and 106 electrodes in the presence of TTX 1 μM and (C) following the addition of CBX 150 μM.



FIGURE 8 | Effect of EGTA on the stimulus-evoked oscillation. (A) Sixty seconds of representative SALPA filtered traces at baseline, with 10 mM EGTA and after washout (five days). 0.5 V stimulus (large black arrowhead). (B) Average power spectra showing baseline with TTX 1 μM and (C) after the addition of 10 mM EGTA. 0.5 V stimulus at time 0 (hippocampal culture, age six weeks, n = 22 electrodes).

by others (Bragin et al., 2002a, 2007). Similarly, high frequency ripple oscillations have been observed and induced in hippocampal slice cultures (Draguhn et al., 1998; Behrens et al., 2005). Interestingly, there is also a less prominent power band above 600 Hz that may represent another pathological oscillation or, since there does appear to be a decrease in power when TTX is added (**Figure 2C**) or in the presence of EGTA (**Figure 8C**), this may just be superimposed multiunit action potentials or perhaps rebounding dAPs. In the average baseline power spectrum (**Figure 2A**), there is also a small brief broad-band increase in power in the oscillation containing electrode just post stimulus on other electrodes. This may be related to stimulus artifact, dAPs or brief multiunit activity causing subtle transient activation of the oscillation. It is also possible that the high frequency oscillation is present even in baseline conditions
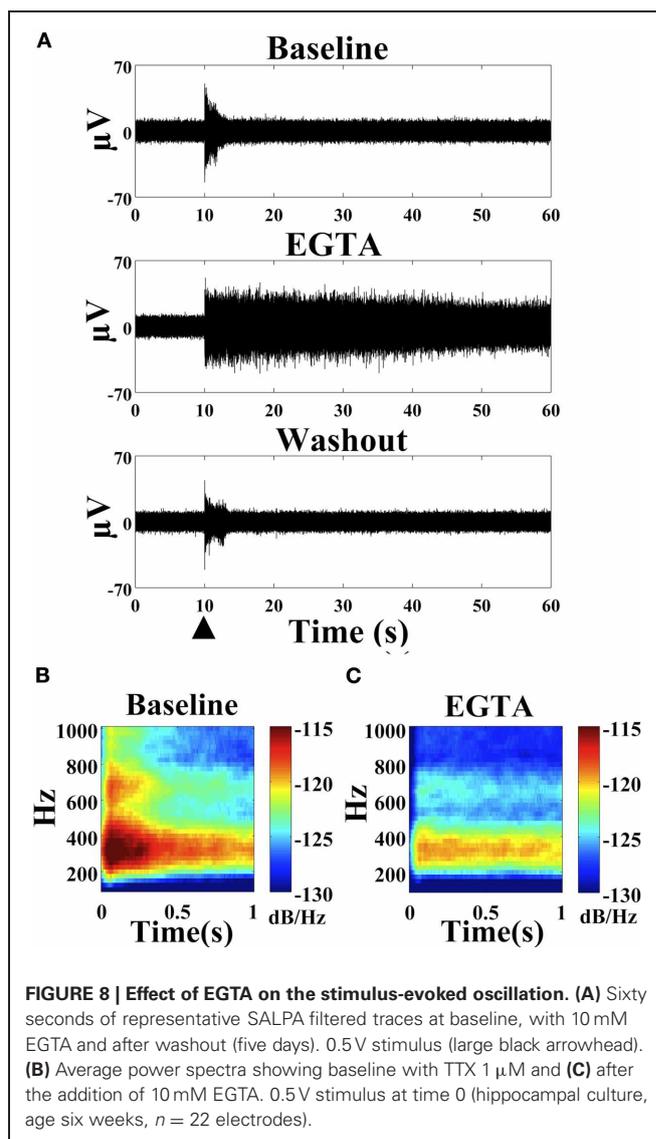
but just low in amplitude until facilitated by an electrical stimulus.

The etiology of pathological high frequency oscillations remains largely unknown, however, work in slice cultures suggests that electrical coupling of cells may be responsible (Draguhn et al., 1998; Traub et al., 2002; Roopun et al., 2010). The continuation of the oscillation in the presence of TTX suggests that the activity is not mediated by voltage-dependent sodium channels. The slight reduction in the oscillation amplitude occasionally observed (**Figure 1B**) in the presence of TTX is likely secondary to a loss of superimposed action potentials present in the TTX treated culture. Alternatively, it is possible that there could also be a minor contribution from sodium currents in facilitating the oscillation. Similarly the use of synaptic blockers demonstrates that glutamatergic or GABAergic activity is likely not responsible for the oscillation. The inhibitory effect of carbenoxolone on the stimulus-evoked oscillation is in agreement with the slice work in suggesting that the

oscillation may be due to electrical coupling from gap junctions. There is controversy in the literature concerning the specificity of carbenoxolone for gap junction blockade (Chepkova et al., 2008; Tovar et al., 2009; Beaumont and Maccaferri, 2011; Behrens et al., 2011), however, the non-specific effects are partially mitigated since the oscillation persists despite synaptic blockade. That the low calcium condition enhances the oscillation is also consistent with a gap junction mechanism, as is the highly localized nature of the activity. Others have demonstrated the presence of gap junctions in the central nervous system and shown that gap junction connections may only transmit signals in highly localized environments (Sohl et al., 2005; Roopun et al., 2010). It is not clear based on these studies whether the activity is mediated by neurons, glia or a combination of cells as cultures utilized for these experiments are mixed neuron/glia cultures.

If the oscillation is mediated by neurons, then axonal processes, direct soma contacts, or some combination may be responsible. With 30 μm electrodes and 25,000–50,000 cells in the dish, there were likely multiple cell bodies in contact with the electrode in addition to hundreds and possibly thousands of cellular processes. Therefore, it is likely that multiple cells are being directly impacted by the stimulation. It would be unlikely for a single-cell to be solely responsible for the extracellular recordings unless perhaps the oscillation is caused by transient membrane damage. The electrical coupling model is feasible and could represent localized transmission through coupled processes or cell bodies. There is likely a limited contribution from synaptic activity given that synaptic blockers were evaluated and that the oscillation was localized to a single electrode and did not spread to adjacent electrodes. Further studies are needed to better characterize the physiological changes, including directed imaging with calcium or pH sensitive dyes as well as intracellular clamping during the oscillations.

This model may prove to be a useful tool for establishing a greater understanding of pathological high frequency oscillations and how they may lead to epilepsy. There could also be applications in studying learning and memory and possible therapies for those with cognitive impairments like Alzheimer's disease, the most common cause of cognitive decline. A clinical trial utilizing carbenoxolone versus placebo demonstrated improved cognitive scores in elderly men (Sandeep et al., 2004). Although the effect was mainly attributed to reductions in glucocorticoid concentrations, an alternative hypothesis based on this work suggests that reductions in pathological high frequency oscillations may also be responsible for the improved cognition. Intriguingly, high frequency oscillations in epilepsy and cognition are intertwined since both patients and animal models with Alzheimer's disease can develop seizures (Palop et al., 2007). Further studies would be needed to explore the mechanism of action at the molecular level and to determine whether or not the effect is merely symptomatic or perhaps disease modifying.

This is the first demonstration of the ability to induce pathological high frequency oscillations in dissociated cultures and these *in vitro* fast ripples may be dependent on electrical coupling. The model may help to elucidate the basic pathophysiological mechanisms of devastating illnesses like epilepsy and Alzheimer's disease. Ultimately, this model may have potential for use in high-throughput pharmacological screens in establishing better therapies for aberrant brain activity.

## REFERENCES

Axmacher, N., Elger, C. E., and Fell, J. (2008). Memory formation by refinement of neural representations: the inhibition hypothesis. *Behav. Brain Res.* 189, 1–8.

Bakkum, D. J., Chao, Z. C., and Potter, S. M. (2008). Long-term activity-dependent plasticity of action potential propagation delay and amplitude in cortical networks. *PLoS ONE* 3:e2088. doi: 10.1371/journal.pone.0002088

Beaumont, M., and Maccaferri, G. (2011). Is connexin36 critical for GABAergic hypersynchronization in the hippocampus? *J. Physiol.* 589, 1663–1680.

Behrens, C. J., Ul Haq, R., Liotta, A., Anderson, M. L., and Heinemann, U. (2011). Nonspecific effects of the gap junction blocker mefloquine on fast hippocampal network oscillations in the adult rat *in vitro*. *Neuroscience* 192, 11–19.

Behrens, C. J., van den Boom, L. P., de hoz, L., Friedman, A., and Heinemann, U. (2005). Induction of sharp wave-ripple complexes *in vitro* and reorganization of hippocampal networks. *Nat. Neurosci.* 8, 1560–1567.

Bragin, A., Azizyan, A., Almajano, J., Wilson, C. L., and Engel, J. Jr. (2005). Analysis of chronic seizure onsets after intrahippocampal kainic acid injection in freely moving rats. *Epilepsia* 46, 1592–1598.

Bragin, A., Engel, J. Jr., Wilson, C. L., Fried, I., and Buzsaki, G. (1999a). High-frequency oscillations in human brain. *Hippocampus* 9, 137–142.

Bragin, A., Engel, J. Jr., Wilson, C. L., Fried, I., and Mathern, G. W. (1999b). Hippocampal and entorhinal cortex high-frequency oscillations (100–500 Hz) in human epileptic brain and in kainic acid–treated rats with chronic seizures. *Epilepsia* 40, 127–137.

Bragin, A., Engel, J. Jr., Wilson, C. L., Vizentin, E., and Mathern, G. W. (1999c). Electrophysiologic analysis of a chronic seizure model after unilateral hippocampal KA injection. *Epilepsia* 40, 1210–1221.

Bragin, A., Engel, J. Jr., and Staba, R. J. (2010). High-frequency oscillations in epileptic brain. *Curr. Opin. Neurol.* 23, 151–156.

Bragin, A., Mody, I., Wilson, C. L., and Engel, J. Jr. (2002a). Local generation of fast ripples in epileptic brain. *J. Neurosci.* 22, 2012–2021.

Bragin, A., Wilson, C. L., Almajano, J., Mody, I., and Engel, J. Jr. (2004). High-frequency oscillations after status epilepticus: epileptogenesis and seizure genesis. *Epilepsia* 45, 1017–1023.

Bragin, A., Wilson, C. L., Staba, R. J., Reddick, M., Fried, I., and Engel, J. Jr. (2002b). Interictal high-frequency oscillations (80-500 Hz) in the human epileptic brain: entorhinal cortex. *Ann. Neurol.* 52, 407–415.

Bragin, A., Wilson, C. L., and Engel, J. (2003). Spatial stability over time of brain areas generating fast ripples

in the epileptic rat. *Epilepsia* 44, 1233–1237.

Bragin, A., Wilson, C. L., and Engel, J. Jr. (2000). Chronic epileptogenesis requires development of a network of pathologically interconnected neuron clusters: a hypothesis. *Epilepsia* 41(Suppl. 6), S144–S152.

Bragin, A., Wilson, C. L., and Engel, J. Jr. (2007). Voltage depth profiles of high-frequency oscillations after kainic acid-induced status epilepticus. *Epilepsia* 48(Suppl. 5), 35–40.

Buzsaki, G., Horvath, Z., Urioste, R., Hetke, J., and Wise, K. (1992). High-frequency network oscillation in the hippocampus. *Science* 256, 1025–1027.

Cardin, J. A., Carlen, M., Meletis, K., Knoblich, U., Zhang, F., Deisseroth, K., Tsai, L. H., and Moore, C. I. (2009). Driving fast-spiking cells induces gamma rhythm and controls sensory responses. *Nature* 459, 663–667.

Chao, Z. C., Bakkum, D. J., and Potter, S. M. (2008). Shaping embodied neural networks for adaptive goal-directed behavior. *PLoS Comput. Biol.* 4:e1000042. doi: 10.1371/journal.pcbi.1000042

Chepkova, A. N., Sergeeva, O. A., and Haas, H. L. (2008). Carbenoxolone impairs LTP and blocks NMDA receptors in murine hippocampus. *Neuropharmacology* 55, 139–147.

Chrobak, J. J., and Buzsaki, G. (1996). High-frequency oscillations in the output networks of the hippocampal-entorhinal axis of the freely behaving rat. *J. Neurosci.* 16, 3056–3066.

Dichter, M. A. (1978). Rat cortical neurons in cell culture: culture methods, cell morphology, electrophysiology, and synapse formation. *Brain Res.* 149, 279–293.

Draguhn, A., Traub, R. D., Schmitz, D., and Jefferys, J. G. (1998). Electrical coupling underlies high-frequency oscillations in the hippocampus *in vitro*. *Nature* 394, 189–192.

Engel, A. K., and Singer, W. (2001). Temporal binding and the neural correlates of sensory awareness. *Trends Cogn. Sci.* 5, 16–25.

Engel, J. Jr., Bragin, A., Staba, R., and Mody, I. (2009). High-frequency oscillations: what is normal and what is not? *Epilepsia* 50, 598–604.

Fell, J., Fernandez, G., Klaver, P., Elger, C. E., and Fries, P. (2003). Is synchronized neuronal gamma activity relevant for selective attention? *Brain Res. Brain Res. Rev.* 42, 265–272.

Fell, J., Klaver, P., Lehnertz, K., Grunwald, T., Schaller, C., Elger, C. E., and Fernandez, G. (2001). Human memory formation is accompanied by rhinal-hippocampal coupling and decoupling. *Nat. Neurosci.* 4, 1259–1264.

Gruber, T., Tsivilis, D., Montaldi, D., and Muller, M. M. (2004). Induced gamma band responses: an early marker of memory encoding and retrieval. *Neuroreport* 15, 1837–1841.

Hales, C. M., Rolston, J. D., and Potter, S. M. (2010). How to culture, record and stimulate neuronal networks on micro-electrode arrays (MEAs). *J. Vis. Exp.* 39. doi: 10.3791/2056

Herrmann, C. S., Munk, M. H., and Engel, A. K. (2004). Cognitive functions of gamma-band activity: memory match and utilization. *Trends Cogn. Sci.* 8, 347–355.

Jacobs, J., Levan, P., Chander, R., Hall, J., Dubeau, F., and Gotman, J. (2008). Interictal high-frequency oscillations (80-500 Hz) are an indicator of seizure onset areas independent of spikes in the human epileptic brain. *Epilepsia* 49, 1893–1907.

Jirsch, J. D., Urrestarazu, E., Levan, P., Olivier, A., Dubeau, F., and Gotman, J. (2006). High-frequency oscillations during human focal seizures. *Brain* 129, 1593–1608.

Jiruska, P., Csicsvari, J., Powell, A. D., Fox, J. E., Chang, W. C., Vreugdenhil, M., Li, X., Palus, M., Bujan, A. F., Dearden, R. W., and Jefferys, J. G. (2010). High-frequency network activity, global increase in neuronal activity, and synchrony expansion precede epileptic seizures *in vitro*. *J. Neurosci.* 30, 5690–5701.

Khosravani, H., Mehrotra, N., Rigby, M., Hader, W. J., Pinnegar, C. R., Pillay, N., Wiebe, S., and Federico, P. (2009). Spatial localization and time-dependant changes of electrographic high frequency oscillations in human temporal lobe epilepsy. *Epilepsia* 50, 605–616.

Madhavan, R., Chao, Z. C., and Potter, S. M. (2007). Plasticity of recurring spatiotemporal activity patterns in cortical networks. *Phys. Biol.* 4, 181–193.

Oostenveld, R., Fries, P., Maris, E., and Schoffelen, J. M. (2011). FieldTrip: open source software for advanced analysis of MEG, EEG, and invasive electrophysiological data. *Comput. Intell. Neurosci.* 2011, 156869.

Palop, J. J., Chin, J., Roberson, E. D., Wang, J., Thwin, M. T., Bien-Ly, N., Yoo, J., Ho, K. O., Yu, G. Q., Kreitzer, A., Finkbeiner, S., Noebels, J. L., and Mucke, L. (2007). Aberrant excitatory neuronal activity and compensatory remodeling of inhibitory hippocampal circuits in mouse models of Alzheimer's disease. *Neuron* 55, 697–711.

Perez-Velazquez, J. L., Valiante, T. A., and Carlen, P. L. (1994). Modulation of gap junctional mechanisms during calcium-free induced field burst activity: a possible role for electrotonic coupling in epileptogenesis. *J. Neurosci.* 14, 4308–4317.

Pimashkin, A., Kastalskiy, I., Simonov, A., Koryagina, E., Mukhina, I., and Kazantsev, V. (2011). Spiking signatures of spontaneous activity bursts in hippocampal cultures. *Front. Comput. Neurosci.* 5:46. doi: 10.3389/fncom.2011.00046

Potter, S. M., and DeMarse, T. B. (2001). A new approach to neural cell culture for long-term studies. *J. Neurosci. Methods* 110, 17–24.

Rolston, J. D., Gross, R. E., and Potter, S. M. (2009). A low-cost multi-electrode system for data acquisition enabling real-time closed-loop processing with rapid recovery from stimulation artifacts. *Front. Neuroeng.* 2:12. doi: 10.3389/neuro.16.012.2009

Rolston, J. D., Gross, R. E., and Potter, S. M. (2010). Closed-loop, open-source electrophysiology. *Front. Neurosci.* 4:31. doi: 10.3389/fnins.2010.00031

Rolston, J. D., Wagenaar, D. A., and Potter, S. M. (2007). Precisely timed spatiotemporal patterns of neural activity in dissociated cortical cultures. *Neuroscience* 148, 294–303.

Roopun, A. K., Simonotto, J. D., Pierce, M. L., Jenkins, A., Nicholson, C., Schofield, I. S., Whittaker, R. G., Kaiser, M., Whittington, M. A., Traub, R. D., and Cunningham, M. O. (2010). A nonsynaptic mechanism underlying interictal discharges in human epileptic neocortex. *Proc. Natl. Acad. Sci. U.S.A.* 107, 338–343.

Sandeep, T. C., Yau, J. L., Maclullich, A. M., Noble, J., Deary, I. J., Walker, B. R., and Seckl, J. R. (2004). 11Beta-hydroxysteroid dehydrogenase inhibition improves cognitive function in healthy elderly men and type 2 diabetics. *Proc. Natl. Acad. Sci. U.S.A.* 101, 6734–6739.

Schevon, C. A., Trevelyan, A. J., Schroeder, C. E., Goodman, R. R., Mckhann, G. Jr., and Emerson, R. G. (2009). Spatial characterization of interictal high frequency oscillations in epileptic neocortex. *Brain* 132, 3047–3059.

Sederberg, P. B., Kahana, M. J., Howard, M. W., Donner, E. J., and Madsen, J. R. (2003). Theta and gamma oscillations during encoding predict subsequent recall. *J. Neurosci.* 23, 10809–10814.

Siapas, A. G., and Wilson, M. A. (1998). Coordinated interactions between hippocampal ripples and cortical spindles during slow-wave sleep. *Neuron* 21, 1123–1128.

Sirota, A., Csicsvari, J., Buhl, D., and Buzsaki, G. (2003). Communication between neocortex and hippocampus during sleep in rodents. *Proc. Natl. Acad. Sci. U.S.A.* 100, 2065–2069.

Sohl, G., Maxeiner, S., and Willecke, K. (2005). Expression and functions of neuronal gap junctions. *Nat. Rev. Neurosci.* 6, 191–200.

Staba, R. J., Wilson, C. L., Bragin, A., Fried, I., and Engel, J. Jr. (2002). Quantitative analysis of high-frequency oscillations (80-500 Hz) recorded in human epileptic hippocampus and entorhinal cortex. *J. Neurophysiol.* 88, 1743–1752.

Staba, R. J., Wilson, C. L., Bragin, A., Jhung, D., Fried, I., and Engel, J. Jr. (2004). High-frequency oscillations recorded in human medial temporal lobe during sleep. *Ann. Neurol.* 56, 108–115.

Tovar, K. R., Maher, B. J., and Westbrook, G. L. (2009). Direct actions of carbenoxolone on synaptic transmission and neuronal membrane properties. *J. Neurophysiol.* 102, 974–978.

Traub, R. D., Draguhn, A., Whittington, M. A., Baldeweg, T., Bibbig, A., Buhl, E. H., and Schmitz, D. (2002). Axonal gap junctions between principal neurons: a novel source of network oscillations, and perhaps epileptogenesis. *Rev. Neurosci.* 13, 1–30.

Ulanovsky, N., and Moss, C. F. (2007). Hippocampal cellular and network activity in freely moving echolocating bats. *Nat. Neurosci.* 10, 224–233.

Urrestarazu, E., Chander, R., Dubeau, F., and Gotman, J. (2007). Interictal high-frequency oscillations (100-500 Hz) in the intracerebral EEG of epileptic patients. *Brain* 130, 2354–2366.

Wagenaar, D. A., Madhavan, R., Pine, J., and Potter, S. M. (2005). Controlling bursting in cortical cultures with closed-loop multi-electrode stimulation. *J. Neurosci.* 25, 680–688.

Wagenaar, D. A., Nadasdy, Z., and Potter, S. M. (2006a). Persistent

dynamic attractors in activity patterns of cultured neuronal networks. *Phys. Rev. E Stat. Nonlin. Soft Matter Phys.* 73, 051907.

Wagenaar, D. A., Pine, J., and Potter, S. M. (2006b). An extremely rich repertoire of bursting patterns during the development of cortical cultures. *BMC Neurosci.* 7, 11.

Wagenaar, D. A., and Potter, S. M. (2002). Real-time multi-channel stimulus artifact suppression by local curve fitting. *J. Neurosci. Methods* 120, 113–120.

Worrell, G. A., Gardner, A. B., Stead, S. M., Hu, S., Goerss, S., Cascino, G. J., Meyer, F. B., Marsh, R., and Litt, B. (2008). High-frequency oscillations in human temporal lobe: simultaneous microwire and clinical macroelectrode recordings. *Brain* 131, 928–937.

**Conflict of Interest Statement:** The authors declare that the research was conducted in the absence of any commercial or financial relationships that could be construed as a potential conflict of interest.